Supplementary Methods

Neural recordings

Neural recordings were made using Pt/Ir electrodes in multiple-electrode microdrives (3- or 5-channel, Thomas Recordings, Germany). Neural activity was referenced to the guide tube in each chamber which was in contact with the cerebral spinal fluid. During each session neural activity from each electrode was passed through a headstage (x20, Thomas Recordings, Germany), filtered (1 Hz – 10 kHz; custom), amplified (x500-1000; TDT Electronics, Gainesville, FL), digitized (20 kHz; National Instruments, TX) and continuously recorded to disk for further analysis (custom C and Matlab code).

At a subset of recording sites in the frontal chamber of each monkey, microstimulation through the recording electrode evoked movements of the hand, arm and occasionally leg with a threshold > 40 uA (330 Hz 400 us monopolar pulse width) consistent with published reports for PMd[1]. With a low amplitude <80 uA pulse, saccades were not evoked at any recording site, consistent with published reports for the caudal subdivision of PMd [2]. Single cell recordings from both areas in both animals contained visual-, delay- and reach-related responses.

It is possible that the phase of the LFP signal is seriously distorted due to electrode polarization and signal conditioning by the recording hardware [3,4]. We confirmed this was not the case for our recordings by recording signals of known phase using an electrode in saline. Plotting the signal at 1 kHz recorded by the electrode in saline against the 1 kHz signal generated by the function generator showed that there was no appreciable phase distortion in the measurement.

Data collection

Spike and LFP recordings: Cells were first isolated and, if stable, recordings proceeded to the free search and instructed search tasks. Occasionally, cells were acquired on additional electrodes and recorded despite the fact that they had no task response, or cells were lost during a recording. All cells that were recorded for a minimum of 100 trials per search task were included in the database regardless of task response. Another database of recordings was obtained during the centre-out task using the same procedure. Recordings during the search tasks and the centre-out task were made in separate blocks of trials.

LFP activity was recorded on electrodes regardless of the presence of spiking activity. If there was no spike activity at a site, online displays of LFP responses to the centre-out task were sometimes used to select recording sites. Occasionally, electrodes were moved significant distances (>200 um) while searching for spiking activity. In contrast, it was sometimes necessary to move electrodes smaller distances (<200 um) to maintain single unit isolations especially during longer recordings. Based on this observation, we defined an LFP recording from a single site as activity recorded on an electrode whose depth did not vary by more than 200 um. Electrode position was continuously logged during the recording and, during post-processing, trials were grouped according to the depth of each electrode using this criterion. All sites that were recorded for a minimum of 100 trials per task were included in the database regardless of task response. LFP activity was filtered from the raw recording by first passing the data through a median filter (duration 1.5 ms) to suppress large amplitude spiking activity, and then low-pass filtering at 300 Hz with a 100 ms filter constructed from Slepian functions. This filter had excellent low-pass filter properties and did not introduce phase distortion. This was verified by visual inspection of both the original broad-band and LFP filtered signals which were seen to overlay each other without distortion. As a result, filtering

did not induce a phase shift relative to the spiking. We recorded from pairs of sites with and without overlapping response fields.

During the search tasks, analysis of spike-field coherence between PRR and PMd was determined from recordings of 84 PMd neurons, 82 PRR LFP sites, 17 PRR neurons, and 20 PMd LFP sites in Monkey E and 64 PMd neurons, 32 PRR LFP sites, 24 PRR neurons, and 26 PMd LFP sites in Monkey Z. During the centre-out task, analysis of spike-field coherence was determined from recordings of a partially-overlapping population of 78 PMd neurons, 69 PRR LFP sites, 41 PRR neurons, and 55 PMd LFP sites in Monkey E and 41 PMd neurons, 38 PRR LFP sites, 38 PRR neurons, and 24 PMd LFP sites in Monkey Z. This population was partially-overlapping because recordings from a minority of neurons and LFP sites were made in both sets of tasks. Results from each animal were pooled. Effects were also significant when data from each animal was treated separately.

Data analysis

Choice entropy: Variability in the movement sequences was quantified by estimating the movement sequence entropy, H, across each of the 56 search array configurations during the free search task. Only trials in which all three movements in the sequence were performed were used. Since rewards were delivered randomly with uniform probability, this procedure provides an unbiased estimate of choice sequence probability distribution. The entropy, H, is given by $H = -\sum_{sequences} p \log_2(p)$ where p is the observed probability of each of the six possible movement sequences. The choice entropy is zero if the same movement sequence is performed every time a search array is presented. The choice entropy is 1 if one of two movement sequences is performed with equal

probability every time a search array is presented. The choice entropy is 1.585 if one of three movement sequences is performed with equal probability. The maximum choice entropy of 2.585 occurs when all six possible movement sequences are performed with equal probability.

Spike sorting was done by extracting and classifying spike events from the broad-band activity using custom Matlab code (Mathworks, Natick, MA) during the recording session. Activity was resorted off-line to confirm isolations. To account for nonstationarity in the recordings, spike classification was done on a 100 s moving window and clusters were tracked across windows. Occasionally there were periods when clusters were not isolated, and trials during those periods were marked. This data was not subject to further analysis.

Spike-field coherence was estimated using multitaper spectral methods with a ±150 ms analysis window with ±15 Hz resolution[5,6]. Coherence is calculated for each frequency band so that, if spike-field coherence is significantly larger than zero, LFP activity at that frequency is correlated with the activity of the neuron. Spike-field coherence may help identify individual neurons that participate in computations across neural circuits. We aligned the analysis window to the time at the centre of the window. As a result, an analysis window that was aligned at stimulus onset included data from a time interval that began before stimulus onset. This "temporal blurring" is necessary to resolve activity at different frequencies but it makes it difficult to compute the latency of spectral responses to stimulus onset and other events in the trial. However, since the blurring affects each spectral estimate in the same way, we can calculate the relative latency of responses between different spectral estimates without problems. Analyses were attempted with a

shorter duration analysis window but there was not sufficient frequency resolution. Frequency resolution is inversely proportional to the temporal duration of the window. Since the effect we observe is at 15 Hz, we believe we are at the limit of the analysis technique.

For all comparisons from a given pair of recording sites, spike-field coherence was estimated on the same number of trials to eliminate estimation bias. Estimates were derived from activity recorded in a total of 100 – 400 trials. Since the firing rate and spectrum varied with movement direction, we estimated coherence for trials to each movement direction and then combined these estimates across movement directions weighted by the number of trials per direction. We included only data from movement directions with at least 20 trials. This procedure allowed us to reliably estimate spike-field coherence from single recording sessions in our data set. The mean response was subtracted from each trace before estimating coherence. Z-scores were determined according to the procedure outlined in Jarvis and Mitra (2001)[7]. This procedure generates a Z-score by calculating the expected standard deviation of the coherence given the number of degrees of freedom (ν = number of trials * number of tapers) and transforming the measured coherence so that, under the null hypothesis that the coherence is zero, the transformed coherence is distributed as a normal variate with variance equal to 1. The transformation we used was $z = \beta(q - \beta)$ where $q = \sqrt{-(\nu - 2) * \log\left(1 - |C|^2\right)}$, $\beta = 1.5$, and C is the coherency.

Partial spike-field coherence let us ask the following questions: Is PMd spiking correlated with PRR LFP activity over and above what we would predict given the correlations between PMd LFP activity and PMd spiking and given the correlations

between PMd LFP activity and PRR LFP activity? Similarly, is PRR spiking correlated with PMd LFP activity over and above what we would predict given PRR LFP activity?

In mathematical terms, partial spike-field coherence uses linear regression analysis in the frequency domain to characterize the relationship between multiple simultaneously-recorded point and continuous processes[8]. Similar to the spike-field coherence, partial spike-field coherence measures the linear dependence between a continuous process, $x(t)$, and a point process, $dN(t)$, but does so after removing the linear contribution of another continuous process, $y(t)$, to either process. It is also possible to define the partial spike-field coherence by removing the linear contribution of another point process to either process, but we do not consider that case here.

Partial coherence is zero when the observed dependence between $x(t)$ and $dN(t)$ is only due to the influence of $y(t)$. Partial coherence is one when $x(t)$ and $dN(t)$ are completely dependent and $y(t)$ is independent of either process. When $y(t)$ is independent of both $x(t)$ and $dN(t)$, the partial spike-field coherence is equal to the spike-field coherence between $x(t)$ and $dN(t)$. Partial spike-field coherence is less than or equal to the spike-field coherence.

We use partial coherence to characterize three simultaneously recorded signals, spiking activity from an area, $dN(t)$, LFP activity recorded from another area, $x(t)$, and LFP activity recorded from the same area as the spiking activity, $y(t)$. The partial coherence between $dN(t)$ and $x(t)$ given $y(t)$ is:

$$C_{XdN|Y}(f) = \frac{C_{XdN}(f) - C_{XY}(f)C_{YdN}(f)}{\sqrt{\left(1-|C_{XY}(f)|^2\right)\left(1-|C_{YdN}(f)|^2\right)}}$$

$C_{XdN}(f)$ and $C_{YdN}(f)$ are the spike-field coherency and $C_{XY}(f)$ is the LFP coherency given by:

$$C_{XdN}(f) = \frac{\left\langle \tilde{X}(f) d\tilde{N}^*(f) \right\rangle}{\sqrt{S_X(f) S_{dN}(f)}}$$

$$C_{YdN}(f) = \frac{\left\langle \tilde{Y}(f) d\tilde{N}^*(f) \right\rangle}{\sqrt{S_Y(f) S_{dN}(f)}}$$

$$C_{XY}(f) = \frac{\left\langle \tilde{X}(f) \tilde{Y}^*(f) \right\rangle}{\sqrt{S_X(f) S_Y(f)}}$$

$S_X(f)$, $S_Y(f)$ and $S_{dN}(f)$ are the spectrum of each process:

$$S_X(f) = \left\langle \left| \tilde{X}(f) \right|^2 \right\rangle$$

$$S_Y(f) = \left\langle \left| \tilde{Y}(f) \right|^2 \right\rangle$$

$$S_{dN}(f) = \left\langle \left| d\tilde{N}(f) \right|^2 \right\rangle$$

$\tilde{X}(f)$, $\tilde{Y}(f)$, and $d\tilde{N}(f)$ are, respectively, the tapered Fourier transforms of $x(t)$, $y(t)$ and $dN(t)$. Above we suppress the indices for trial, (tr), and taper, (k), for notational convenience. * denotes the complex conjugate and $\langle\ \rangle$ denotes the expectation, or average, over trials and windowed Fourier transforms.

To estimate partial coherence, we estimated all spectral quantities using multitaper spectral methods with a ±150 ms analysis window with ±15 Hz resolution.

Supplementary Fig 9 presents a schematic of the partial spike-field coherence analysis to illustrate how we applied it to our problem. We used partial spike-field coherence to test whether spike-field coherence between PRR and PMd could result from

a combination of spike-field coherence within PMd and PRR and LFP coherence between PRR and PMd. Intuitively, this test models the spike-field correlation between areas as being the result of correlations in the LFPs between the two areas combined with the correlation between LFPs and spiking in just one area. According to this model, if spiking is coherent with local LFP activity and if local LFP activity is coherent with LFP activity in another area, coherence between spiking and LFP activity in another area could be a reflection of the coherence in LFP activity across the circuit and not directly due to coherence between spiking and LFP activity across the circuit. The partial spike-field coherence analysis determines if the coherence in the data exceeds the predictions from this model to specifically test how LFP activity in two areas contributes to spike-field coherence between those areas.

The goal of this analysis is to determine how tightly our observations of PMd – PRR spike-field coherence can be linked to the activity of a single neuron across the circuit. The alternative is that LFP coherence is sufficient to characterize neural coordination between the two areas. According to the alternative, we measure correlations in the activity of a single neuron across the circuit because the activity of that neuron is correlated with a local population of neurons whose activity, in turn, can be measured using LFP activity. Simply put: Can our measurements of neural coordination be made using LFP activity alone?

Spiking onset latency was estimated by detecting the time after search array onset during which the average response, estimated on a 20 ms binning interval, was three standard deviations greater than baseline activity for at least 50 ms. Responses were estimated when at least one of the search array elements was in the response field of the cell. Significant differences in response latency were determined using the following

permutation procedure: We shuffled the order of the peri-stimulus spike histograms from free search and instructed search tasks and randomly assigned each recording to one of two new classes. Recordings were assigned to one of the two new classes with the same proportion of recordings in free search and instructed as in the original data set. We then estimated the difference in response latency between the new, shuffled classes using the procedure above. This was repeated 4000 times to generate a null distribution of differences for each comparison between free search and instructed search. The observed difference in response latency between free search and instructed search was compared with this null distribution to assess significance. The reported significant differences in response latency were also obtained when the threshold was varied up to six standard deviations, when the binning interval was reduced to 5 ms and when latency was determined from time of the maximum first derivative of the response.

ROC analysis was performed for firing rate of spiking activity in each area to measure the amount of information about the first movement choice that was present in single neuron activity as a function of time during the trial. ROC analysis measures the discriminability of two alternatives by an ideal observer. This analysis measures the 'choice probability', which is the probability an ideal observer can correctly predict the movement choice from the neuronal activity on each trial. Since we presented three targets, we used ROC analysis to analyze a subset of trials when the monkey chose one of two targets. That is, for each cell, we defined two targets, a preferred target which elicited the most activity and a non-preferred target which elicited less activity and asked how well spiking activity predicted which of these two targets the monkey would chose to reach to. Activity in trials when the other target was selected was not analyzed. This procedure did not omit many trials because of biases in the choice strategy. These biases meant that two of the three targets were usually preferred compared with the third and, as

a result, supported the use of ROC analysis. The analysis was done using a 100 ms analysis window stepped 10 ms between estimates. Only targets for which the cell under study was recorded for 10 trials or more were considered for this analysis. Note that our definition of uncorrelated neurons groups cells which are not correlated with activity in the other area together with cells whose correlations we did not observe.

LFP onset latency was estimated by detecting the time after search array onset during which the average response was three standard deviations greater than baseline activity for at least 50 ms. Significant differences were determined using the same permutation procedure used for determining significant spike response latency differences. The reported significant differences in response latency were also obtained when the threshold was varied up to six standard deviations.

Spatial tuning was determined by calculating the trigonometric moment of the tuning curve[1]. In the case of spiking, the trigonometric moment corresponded to weighting the contribution from a specific direction by the firing rate in that direction and averaging across all directions in the curve. In the case of LFP activity, the integrated power from 1-100 Hz was used. This was dominated by the power present below 20 Hz. Statistical significance was determined using a permutation test. For this test, activity from all trials was shuffled so that the direction of the upcoming movement for a given trial was assigned by drawing randomly from the pool of trials, and the trigonometric moment was re-estimated. This was repeated 4000 times to give a null distribution, and the observed trigonometric moment was compared with this null distribution to determine the level of significance.

Supplementary Results

Reward expectancy

Although we matched reward frequencies between the tasks, other differences between the tasks could lead to differences in reward expectancy. Since reward expectancy modulates activity in both frontal and parietal cortex, it was important to test whether it was, in fact, matched between tasks. Increased reward expectancy reduces the reaction time to movement onset [9], so we tested whether reward contingencies varied between tasks by analyzing the reaction time of each reach in the sequence for 95 behavioural sessions in two monkeys. Consistent with an increase in reward expectancy as the search progressed, we found that reach reaction times decreased as each monkey eliminated targets in the search array (Supplementary Fig. 2; 1^{st} reach - 2^{nd} reach: $p<10^{-23}$ (Wilcoxon); 2^{nd} reach - 3^{rd} reach: $p<10^{-8}$). Importantly, reach reaction times were the same in each task for each reach (1^{st} reach reaction time: Instructed = 481±11 ms; Free = 472±11 ms (p=0.52, Wilcoxon). 2^{nd} reach: Instructed = 330±6 ms; Free = 322±6 ms (p=0.33). 3^{rd} reach: Instructed = 273±7 ms; Free = 277±6 ms (p=0.98) Mean±s.e.m). Since reaction times did not vary between the free search and instructed search tasks, we concluded that movements in the two tasks were consistent with similar reward expectancy. This result implies that each monkey closely followed the instructions. Consistent with this, errors in following the instructions during the instructed task occurred very rarely (<1 error per 1000 trials).

Free search choice behaviour

We found that an important property of each free search strategy was that the probability of choosing to reach to a given target first depended on its spatial location. This is illustrated for one monkey in Supplementary Fig. 3, which shows the spatial organization of this bias. This means that the outcome of the choice process depends on locations of the other targets in the array. Supplementary Fig. 3b, demonstrates that the probability of a target being chosen first varies over the course of 57 sessions for one monkey. This also shows that the biases fluctuate over the course of the experiment sessions.

Constant variation in the biases meant that even the strongest biases did not become engrained in the behaviour. We wanted to characterize how variable the movement sequence choices were in the free search task. Supplementary Fig. 3c,d shows the distribution of choice entropies for each monkey across all search array configurations. We found that during free search, responses were not stereotyped and on average were evenly distributed between two or three different sequences.

The variability in chosen sequences during free search was due to the relatively large number of search array configurations we presented, which could have made it difficult for either monkey to develop strong biases. When we reduced the number of search array configurations to one, each monkey quickly chose to perform a single, stereotyped movement sequence.

Other differences between the tasks

Analyzing behaviour during the search tasks suggests that, while they could require differing amounts attention or effort, the major difference between the tasks relates to decision making. The number of saccades and their endpoints did not significantly differ between the tasks, suggesting that demands on spatial attention were similar in each case (see Eye movements below). We also found error rates for the instructed search task were remarkably low (< 0.1 %) and reaction times for each task were similar (see Reward expectancy above). This indicates that, with practice, the animals did not find one task much more difficult than the other.

Eye movements

In the period after the search array was presented and before the first reach, each monkey made a number of saccadic eye movements. These saccades typically scanned the targets present on that trial. To determine whether the gross properties of these eye movements differed between free choice and instructed behaviours, we compared the number of eye movements made during the delay period before the first reach choice in each task. We found that the mean number of saccades was 4.3±0.6 saccades in the free search task and 4.1±0.7 saccades in the instructed search task. The difference in the number of saccades was not significantly different between the tasks ($p = 0.43$; t-test). We also calculated the amount of time each monkey spent fixating the target locations during the 300 ms following search array onset and found that saccade endpoints did not differ significantly between the free search and instructed search tasks ($p = 0.16$, chi-squared test). These analyses indicate that, overall, similar eye movements were made during each task and so overall differences in gaze could not account for the observed effects. Since differences

in the allocation of spatial attention would lead to differences in eye position, this suggests that demands on spatial attention were similar in each task.

Spike-field coherence was significant in the period several hundred milliseconds following search array onset, so we analyzed the latencies of saccades made at this time. On around 90% of trials or more, each monkey made a saccade within 500 ms of the onset of the search array (Monkey E, p =0.97. Monkey Z, p=0.88). In one animal, (Monkey E) the latency of saccades during free search was significantly longer than the latency during instructed search (Free search latency = 290 ms; Instructed search latency = 232 ms. $p<10^{-12}$ (Wilcoxon rank test)). However, in the other animal (Monkey Z), the difference in saccade latency between tasks was not significant (Free search latency = 234 ms; Instructed search latency = 221 ms. p=0.10 (Wilcoxon rank test)). This may be due to the relatively small number of sessions in this animal (15 sessions for Monkey Z compared with 53 sessions for Monkey E).

Influence of eye movements on spike-field coherence

The presence of reliable saccades following search array onset raises the possibility that the spike-field coherence we observe is due to these eye movements. To test whether spike-field coherence was due to these eye movements, we performed another experiment in one of the animals (Monkey E) in which he performed a variant of the search tasks that involved enforced fixation. In this variant, eye movements were not allowed immediately following search array onset and were only allowed at the time of each reach movement. We defined a database of 111 PMd spike – PRR field recordings and 58 PRR spike – PMd field recordings. These recordings showed essentially the same pattern of spike-field coherence that we observed in the search tasks without enforced fixation

(Supplementary Fig. 5 and Supplementary Tables 1 and 2). Spike-field coherence was significant following search array onset even during fixation and was stronger during free search than instructed search. Since spike-field coherence was very similar during a variant of each search task with enforced fixation, the reliable saccades made following search array onset do not drive PMd – PRR coherence.

Influence of reaching on spike-field coherence

We also observed some spike-field coherence between PMd and PRR during the reaching movement. This coherence was strongest between spiking in PRR and LFP activity in PMd and peaked during the reach movement. Coherence at this time likely does not reflect decision making and instead reflects the processes related to executing the reaching movement such as the movement command and subsequent online control of the movement.

Phase histograms of spike-field correlations between PMd and PRR

Spike-field coherence between PMd and PRR may be a result of correlations in the timing of activity in each area. If this is true and the timing of activity in each area is correlated with that in the other, the relative phase of activity in each area at a given frequency, 15 Hz in this case, will show a preferred phase. For the example recordings shown in Fig 2, we plotted the histogram of the relative phase of activity in each area in the 300 ms following search array onset in order to directly examine correlations in the timing of each signal, independent from their amplitude (Supplementary Fig 4). We

found that PMd spiking and PRR LFP activity had a preferred phase during both free and instructed search (Supplementary Fig 4a,b Left panels. Free: Phase = -123°, $p<10^{-9}$; Instructed: Phase = -131°, $p<10^{-4}$. Rayleigh test). In the case of PRR spiking and PMd LFP activity, the distribution of phase differences was unimodal during free search (Supplementary Fig 4c. Left panel. Phase = -121°, $p<0.01$) but not instructed search (Supplementary Fig 4d Left panel. $p=0.44$). This was consistent with the spike-field coherence and showed that correlations in the timing of activity in PMd and PRR following search array onset contribute to spike-field coherence we observe.

However, the onset of the search array leads to activity in PMd and PRR with some latency. Since both areas respond to this stimulus, correlations in their response times may be present even when, on a given trial, the areas are responding independently from each other. We can test whether the preferred phase we observe would be expected from the onset of the stimulus even if PMd and PRR respond independently on a given trial by performing a control analysis. In this analysis, we estimate the relative phase histogram after shuffling the order of the trials for the LFP, without changing the order of the trials for the spiking. We shuffled only the order of trials within free and instructed search and did not shuffle free and instructed trials together. This manipulation preserved the timing of signals locked to search array onset for each trial condition, effectively simulating the expected response when we assume PMd and PRR respond independently. We found that the distribution of shuffled phase differences between PMd spiking and PRR LFP activity did not have a preferred phase in either task (Supplementary Fig. 4a,b. Right panels. $p=0.65$; $p=0.43$, Kuiper's test). Shuffled PRR spiking and PMd LFP activity also did not have a preferred phase (Supplementary Fig 4c,d Right panels. $p=0.11$; $p=0.31$, Kuiper's test).

This results means that responses in PMd and PRR covary across trials so that their timing shows a preferred relative phase. The control analysis shows that this timing relationship is not simply reflected in the response time of each area to the search array onset. Note that this analysis assumes that the trial-by-trial variability of the neural response to the search array onset is smaller than the duration of a 15 Hz cycle (67 ms). This is a reasonable assumption for area LIP[10], a region neighbouring PRR, but remains to be tested for premotor cortex.

In agreement with the coherency analysis, across the population, the phase histograms revealed that both types of spike-field correlations at 15 Hz featured a preferred phase (55/314 (17%) PMd spike – PRR field recordings. 35/187 (19%) PRR spike – PMd field recordings. $p<0.05$, Rayleigh test). Activity at other frequencies and times during the instructed delay period was not significant.

Across the population, analysis of trial-shuffled phase histograms also confirmed that this coherence was not simply due to time-locked common input. After trial-shuffling, almost all PMd spike - PRR field recordings and PRR spike- PMd field recordings had a uniform phase distribution and so did not have a preferred phase at 15 Hz. During free search, phase distributions for only 23 of 314 (7%) PMd spike – PRR field recordings and 10 of 187 (5%) PRR spike – PMd field recordings were significantly non-uniform ($p<0.05$, Kuiper's test). Trial-shuffled phase distributions during instructed search were similarly uniform. Only 24/314 (7%) PMd spike – PRR field phase histograms were non-uniform and 10/187 (5%) PRR spike – PMd field phase histograms were non-uniform ($p<0.05$, Kuiper's test).

Spike-field coherence within PMd and PRR

We investigated spike-field coherence within area PRR and PMd to both understand how spike-field coherence between these areas depended on LFP activity within each area and determine whether within-area coherence was activated by free search. Supplementary Fig. 7 shows an example of spike-field coherence for an example recording in PRR (Supplementary Fig 7a) and PMd (Supplementary Fig 7b) during free search. Two major patterns of correlation are present in these data. Spiking in both areas shows strong persistent correlations with the locally-recorded LFP in a broad 25-45 Hz frequency band. This correlation is prominent during the baseline period before search array onset and during the later part of the delay period before movement and is suppressed both immediately following search array onset and during movement. In addition to this relatively high frequency oscillation, transient low frequency coherence is present immediately following search array onset, most prominently in PMd.

This pattern was present across a population of spike-field recordings within each area (Supplementary Fig 8). During free search, of 397 recordings in PMd, 192 contained significant coherence at 15 Hz immediately following search array onset (48%; $p<0.05$, Permutation test) and 141 (35%) contained significant delay period coherence at 30 Hz. Of 173 recordings in PRR, 81 (47%) contained significant coherence at 15 Hz following search array onset and 117 (68%) contained significant delay period coherence at 30 Hz during free search.

During instructed search, the prevalence of spike-field coherence within each area was surprisingly similar to that observed during free search. 145 of 397 (36%) PMd recordings contained significant 30 Hz delay period coherence during instructed search (36%). 93 of 173 (54%) PRR recordings contained significant 15 Hz coherence

following search array onset. 106 of 173 (61%) PRR recordings contained significant 30 Hz delay period coherence. Each of these proportions for instructed search was not significantly different from the fraction observed in the corresponding data during free search (30 Hz PMd: p=0.76. 15 Hz PRR: p=0.20. 30 Hz PRR: p=0.22. Chi-squared test). The one exception to this pattern of within area coherence was that, during instructed search, only 160 of 397 (40%) PMd recordings were significantly coherent at 15 Hz immediately following search array onset. Although a small difference in percentage, this was significantly less than the corresponding proportion of coherent PMd recordings during free search ($p<0.05$. Chi-squared test).

Spiking activity within PMd and PRR is, therefore, not only correlated with activity in the other area, but also shows a rich dependence on LFP activity recorded in the same area. Free search leads to stronger correlations in PMd spiking with LFP activity across the frontal-parietal circuit. In contrast, only correlations between PRR spiking and LFP activity in PMd are activated by free search, albeit weaker than PMd spiking, and correlations within PRR do not depend on the type of search. The effects of free choice in this circuit appear transient so that correlations within PMd and PRR are equally strong during the delay period before free and instructed movements. This may be because the decision has been made and a movement to the selected target is now being planned.

Partial spike-field coherence between PMd and PRR

The presence of robust within-area spike-field coherence we report above could mean that the between-area spike-field coherence we observe is, effectively, an indirect result of long-range correlations in LFP activity. Alternatively, between-area spike-field coherence may reflect a specific relationship between the activity of an individual neuron

to the LFP activity in another area. We estimated partial spike –field coherence (see Supplementary Methods) to distinguish between these alternatives and test whether recordings of LFP activity in PMd and PRR could explain our observations of spike-field coherence between these areas.

From our database of 74 PMd spike – PRR field recordings with significant 15 Hz coherence immediately following search array onset, we were able to define 190 recordings with an additional LFP recording in PMd on another electrode. Of these 190 simultaneous recordings of spiking in PMd and LFP activity in both PMd and PRR, 140 recordings (74%) had significant PMd spike – PRR field partial coherence during free or instructed search after PMd LFP activity was accounted for ($p<0.05$, t-test). This means that while LFP activity within PMd could account for some of the significant PMd spike – PRR field coherence, a significant amount of spike-field coherence we observed could not be explained by PMd LFP activity.

Analysis of PRR spike – PMd field partial coherence yielded similar results. From the 43 PRR spike – PMd field recordings with significant 15 Hz coherence immediately following search array onset, we defined 101 recordings with an additional LFP recording in PRR. 70 of the 101 recordings (70%) had significant PRR spike- PMd field partial coherence during either search task after PRR LFP activity was accounted for ($p<0.05$; t-test). Therefore, PRR LFP activity did not account for the observed PRR spike – PMd field coherence.

Spike response latency analysis

When we directly compared response latencies between areas, we found that PMd activity in a population of cells preceded PRR activity in both search tasks (PMd free search – PRR free search = 30 ms (Permutation test, $p<0.01$); PMd instructed search – PRR instructed search = 26 ms, ($p<0.05$)); Main Fig 3e).

A smaller number of PRR cells were recorded during the search tasks than during the centre-out task as well as from PMd. To test whether the number of cells in the database influenced the estimate of onset latency across the population, we randomly selected 40 cells from the larger database of recordings and compared the onset latency estimate. We found that, on average, reducing the number of cells in the database from 120 cells to 40 cells increased the estimate of onset latency by less than 5 ms and did not alter the statistical significance of these findings.

Spike response rate analysis

Our database contained 93 PMd cells and 37 PRR cells that showed spatially-tuned activity following search array onset ($p<0.05$). We analyzed the activity of these cells to determine whether they also showed a difference that was selective for the type of search task. We analyzed the firing rate for PMd and PRR neurons during the free search and instructed search tasks before movements to the preferred direction of each cell. We found a majority of neurons showed no significant selectivity for the free search task compared with the instructed search task for individual cells in PMd or PRR. In PMd, 76/93 cells (82%) had the same firing rate during each task ($p>0.05$, Wilcoxon). In PRR, 27/37 cells (73%) had the same firing rate during each task. This shows a minority of

cells show a difference in the overall spike rate between the two tasks. In PMd, of the 17 cells that showed a significant difference in firing between free search and instructed search, 9 cells (53%) had greater activity during free search and 8 cells (47%) had greater activity during instructed search. In PRR, of the 10 cells that showed a significant difference in firing between free search and instructed search, 4 cells (40%) had greater activity during free search and 6 cells (60%) had greater activity during instructed search.

LFP latency analysis

To further characterize the responses of each area to search array onset, we defined a database of 188 PMd and 157 PRR LFP recordings during both search tasks and analyzed the LFP response evoked by search array onset. The evoked LFP response in PMd was significantly different between the free search and instructed search tasks both in the latency (Supplementary Fig 10a. Free = 83 ms; Instructed = 74 ms) and in the overall waveform ($p<0.05$; two tailed t-test). In contrast, the evoked LFP response in PRR did not differ between tasks in either the overall waveform or the latency (Supplementary Fig 10b. Free = 80 ms; Instructed = 82 ms; $p=0.44$, t-test). This result reinforced the distinction that PMd responded earlier and selectively depending on the search task, while PRR did not.

Supplementary Discussion

Interpretation of spike-field measurements

Our data show how spiking and LFP activity can offer complementary perspectives on distributed neural processes. Since the correlations we observe are not simply due to stimulus-locked common input and cannot be explained by LFP activity alone, they may reflect the activity of single neurons across a circuit. While we do not explicitly test the mechanistic relationship between spiking and LFP activity, the strong interpretation of our results is that spiking in a sub-population of neurons in PMd can drive a component of LFP activity in PRR. The same is true for PRR spiking and PMd LFP activity. This may be because spiking generates synaptic potentials in the projection zone and LFP activity reflects dendritic input. This synaptic input may end on inhibitory interneurons which control the oscillatory activity within the local cortical circuitry, leading to a boost in spike-field coherence[11]. Since we also find local spike-field coherence, other components of LFP activity reflect the activity of nearby neurons. Local spike-field coherence could either be because these neurons are being driven to fire by synaptic inputs or because spikes from these neurons themselves drive synaptic inputs to other nearby neurons. More information on the different biological sources of LFP activity and their relationship to the activity of single neurons is needed to resolve these issues.

How long does the decision take?

Our results indicate that the period of strongest communication between PMd and PRR occurs in the first several hundred milliseconds following search array onset. If this communication underlies decision making, it implies that the decision is made within this

relatively short time period. This is reasonable because the search tasks we used involve a simple spatial decision, the sensory stimuli are easily localized and discriminated and the reward structure does not encourage deliberation. Removing the delay following search array onset could help test whether the decision is indeed made within the first few hundred milliseconds. Without a delay, we would expect movements to start after the spike-field coherence we observe, at least 300-400 ms following search array onset. Given that there is no spike-field coherence during the delay, we would also expect that eliminating the delay leads to the same distributions of movement choices we observe with delay. Conversely, making the decision more difficult by increasing the number of targets, making them harder to distinguish, or adjusting their relative value may increase the amount of time it takes to make the decision. If spike-field coherence underlies the decision, we would expect this manipulation will also increase the duration of spike-field coherence between PMd and PRR.

Supplementary References

1 Crammond, D. J. & Kalaska, J. F. Modulation of preparatory neuronal activity in dorsal premotor cortex due to stimulus-response compatibility. *J. Neurophysiol.* 71, 1281-1284 (1994).

2 Fujii, N., Mushiake, H. & Tanji, J. Rostrocaudal distinction of the dorsal premotor area based on oculomotor involvement. *J. Neurophysiol.* 83, 1764-1769 (2000).

3 Nelson, M. J., Pouget, P., Nilsen, E. A., Patten, C. D. & Schall, J. D. Review of signal distortion through metal microelectrode recording circuits and filters. *J. Neurosci. Methods*, doi:1-/1-16/j/jneumeth.2007.2012.2010 (2008).

4 Grimnes, S. & Martinesen, O. G. *Bioimpedance and Bioelectricity Basics*. (Academic Press, 2000).

5 Mitra, P. P. & Pesaran, B. Analysis of dynamic brain imaging data. *Biophys. J.* 76, 691-708 (1999).

6 Pesaran, B., Pezaris, J. S., Sahani, M., Mitra, P. P. & Andersen, R. A. Temporal structure in neuronal activity during working memory in macaque parietal cortex. *Nat. Neurosci.* 5, 805-811 (2002).

7 Jarvis, M. R. & Mitra, P. P. Sampling properties of the spectrum and coherency of sequences of action potentials. *Neural Comput.* 13, 717-749 (2001).

8 Halliday, D. M. *et al.* A framework for the analysis of mixed time series/point process data--theory and application to the study of physiological tremor, single motor unit discharges and electromyograms. *Prog. Biophys. Mol. Biol.* 64, 237-278 (1995).

[9] Watanabe, M. *et al.* Behavioral reactions reflecting differential reward expectations in monkeys. *Exp. Brain Res.* 140, 511-518 (2001).

[10] Bisley, J. W., Krishna, B. S. & Goldberg, M. E. A rapid and precise on-response in posterior parietal cortex. *J. Neurosci.* 24, 1833-1838 (2004).

[11] Buzsaki, G. *Rhythms of the brain*. (Oxford University Press, 2006).

Supplementary Figure 1

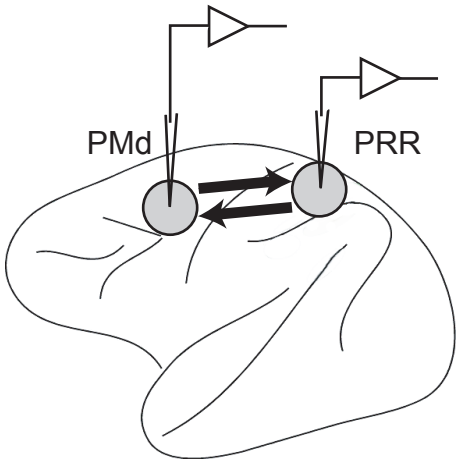

Supplementary Figure 1: Schematic of locations of PMd and PRR with respect to sulcul landmarks. Spiking and LFP activity were simultaneously recorded from electrodes in these areas and referenced to a local ground in each recording chamber. Arrows indicate cortico-cortical projections between these areas.

Supplementary Figure 2

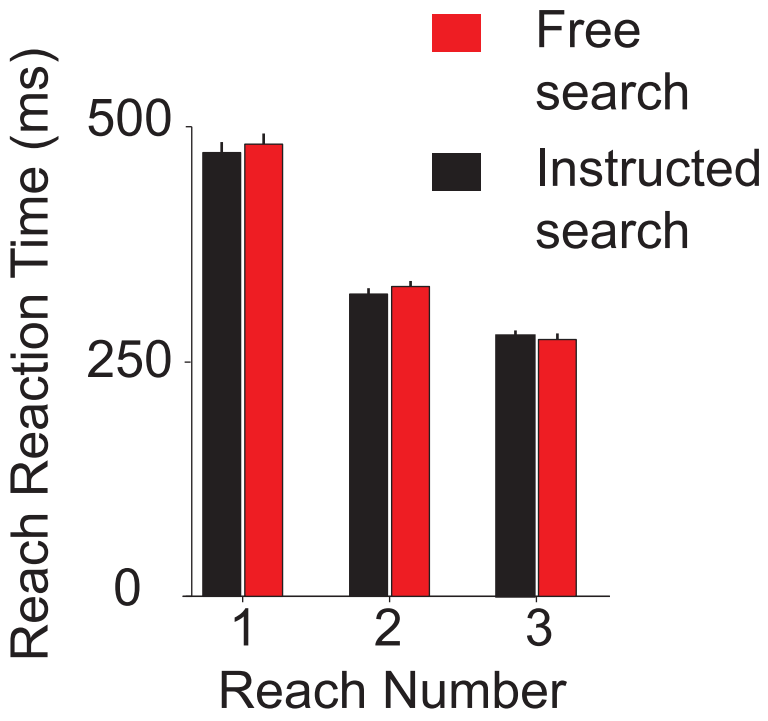

Supplementary Figure 2: Control for reward expectancy. Reach reaction times from the auditory go signal to the time of reach onset. Reaction times are shown for each of the three reaches in the movement sequence for each task. As expected from increased reward expectancy, reaction time decreased as the search progressed. Reaction times in the free search task we not significantly different from those in the instructed search task indicating reward expectancy was matched between each task.

Supplementary Figure 3

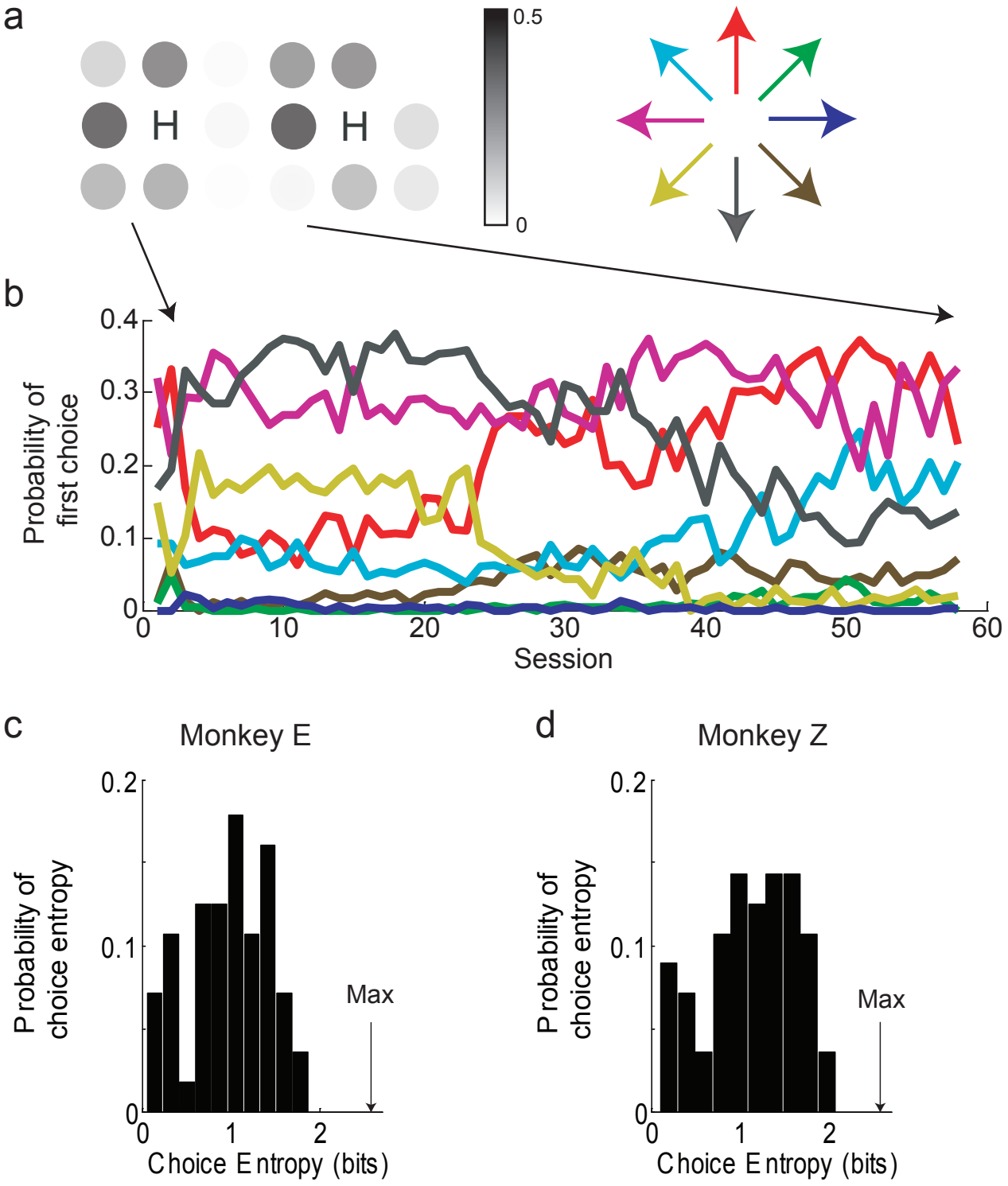

Supplementary Figure 3: Choice behaviour during free search. **a,** Shaded circles giving the probability of choosing each target for the first movement averaged across all search array configurations for a individual sessions. The black arrows indicate which individual session the data is being shown for in **b**. The left panel is for an early session and the right panel is for a late session. **b**, Line plots showing how the probability of choosing a target for the first movement changes between behavioural sessions. Different targets are shown by different coloured lines. The coloured arrows above indicate which colour is used for the different targets. **c**, Distribution of choice entropies for movement sequences elicited by each search array configuration for Monkey E. The arrow labelled 'Max' indicates the maximum choice entropy of 2.585. **d**, Same as **c** for Monkey Z.

Supplementary Figure 4

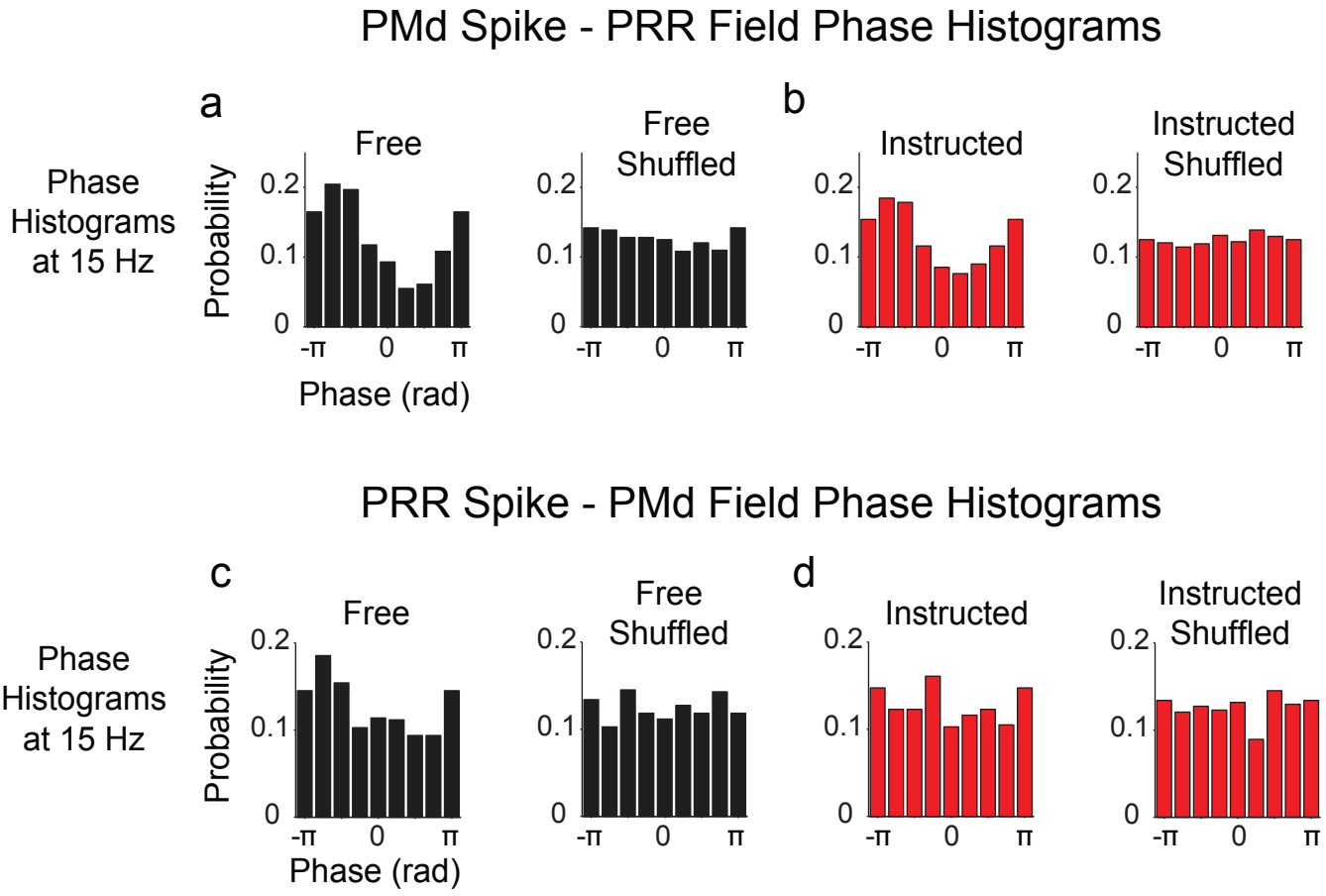

Supplementary Figure 4: Phase analysis for example spike-field recordings in Fig 2. **a)** Histogram of the relative phase between PMd spiking and PRR LFP activity at 15 Hz in the free search task during 300 ms following search array onset. Left panel: Original data. Right panel: Trial-shuffled data. The original data contains a preferred phase difference between spiking and LFP activity. Trial-shuffling, which leaves only stimulus-locked correlations, does not show a significant phase difference. This demonstrates significant spike-field coherence is due to relative timing between spiking and LFP activity and not the timing of their response to search array onset. **b)** PMd spike – PRR field relative phase histogram in the instructed search task. **c)** PRR spike – PMd field relative phase histograms in the free search task. **d)** PRR spike – PMd field relative phase histograms in the instructed search task. In all cases, relative phase histogram at 15Hz does not show a significant phase difference after trial shuffling.

Supplementary Figure 5

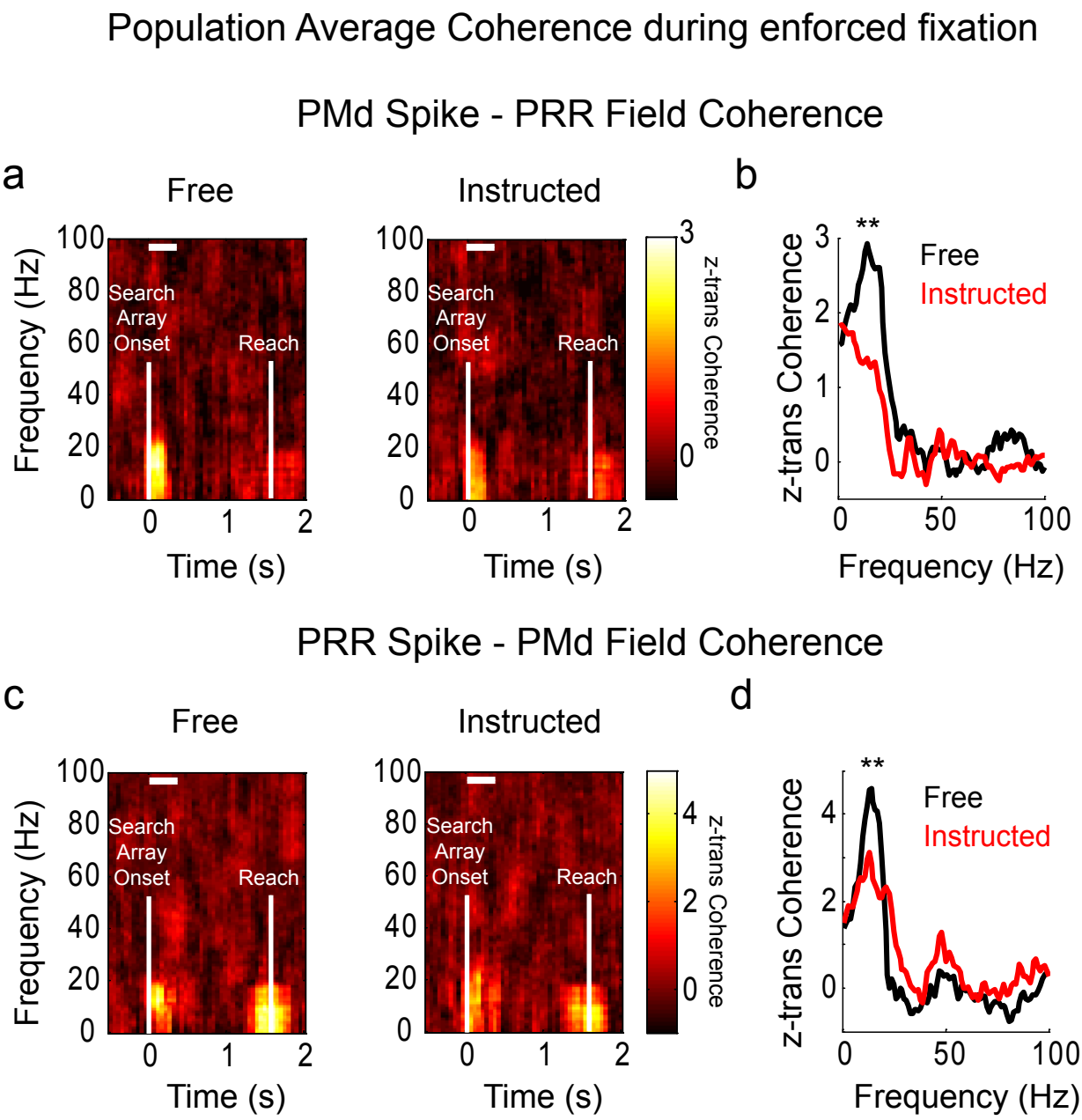

Supplementary Figure 5: Population average PMd – PRR spike-field coherence during search tasks with enforced fixation. Only recordings with significant coherence in either free or instructed search (tabulated in **Supplementary Tables 1 and 2**) with enforced fixation are included in the average, as for Fig 2e. Activity is aligned to the time of search array onset (First vertical white bar). Average time of the 1st reach is shown (Second vertical white bar). Coherence values are z-transformed according to the number of degrees of freedom in the estimate to assess significance and then averaged across the population. Estimates are shown every 50 ms. **a**) Average PMd spike – PRR field coherence during the free and instructed search tasks, respectively. The white horizontal bar indicates the analysis window for data shown in **b**. **b**, Line plots of coherence for free (black) and instructed (red) search tasks during the 300 ms immediately following search array onset. Coherence at 15 Hz is highly significant and greater for free search than instructed search. Activity at other frequencies is not. ** marks the significant difference between free and instructed search ($p<0.05$; t-test). **c-d**, Population average PRR spike – PMd field coherence. The pattern of coherence during search with enforced fixation is the same as during search without enforced fixation (Fig 2). This means that coherence in the search tasks is not due to saccadic eye movements made following search array onset.

Supplementary Figure 6

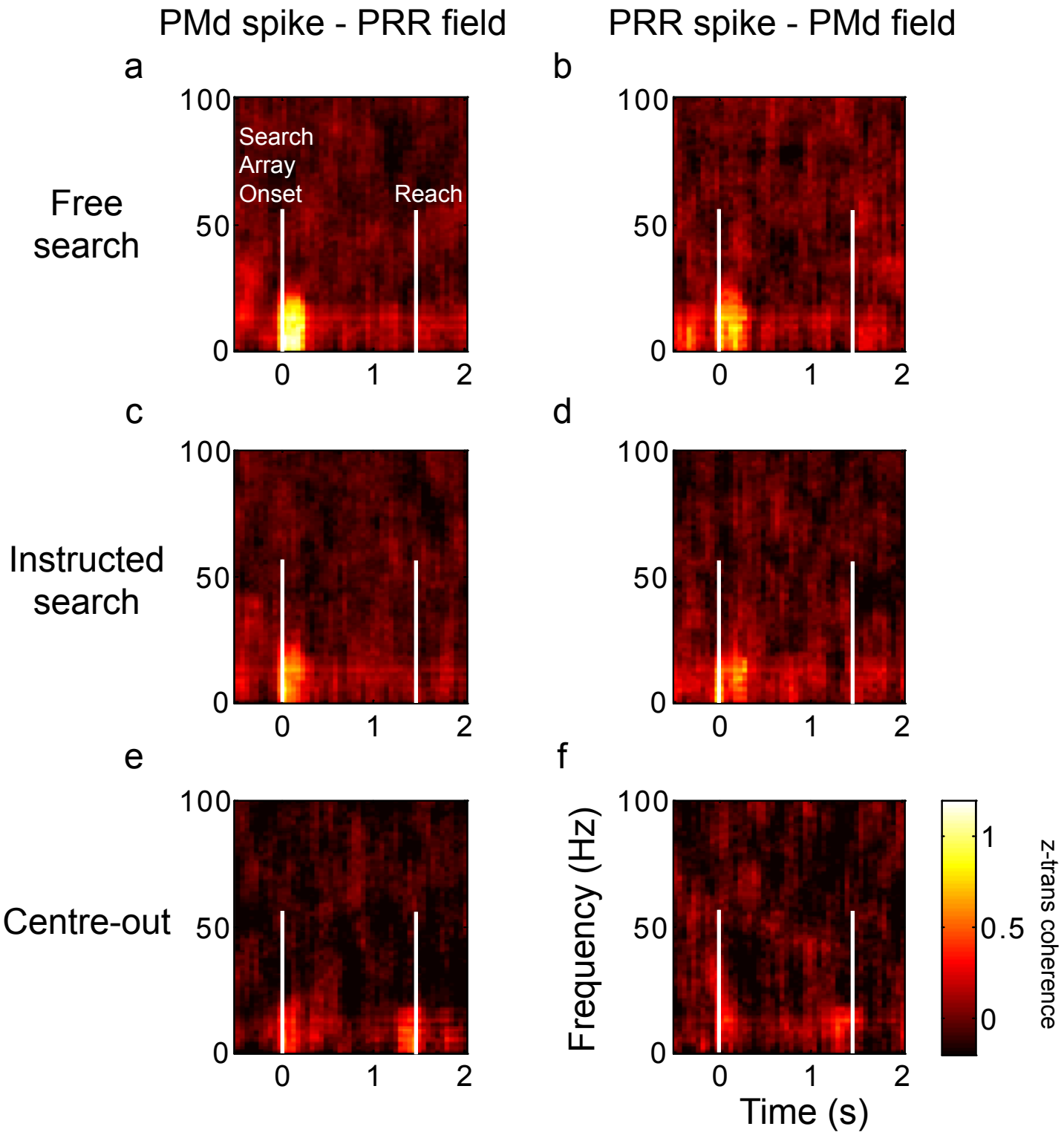

Supplementary Figure 6: Population PMd – PRR spike-field coherence averaged across all sites recorded during free search (a-b), instructed search (c-d) and centre-out (e-f) tasks, irrespective of task response. Coherence values are z-transformed according to the number of degrees of freedom in the estimate to assess significance and then averaged across the population. PMd spike – PRR field and PRR spike – PMd field coherence following search array onset is greater during free search than during instructed search and least in the centre-out task.

Supplementary Figure 7

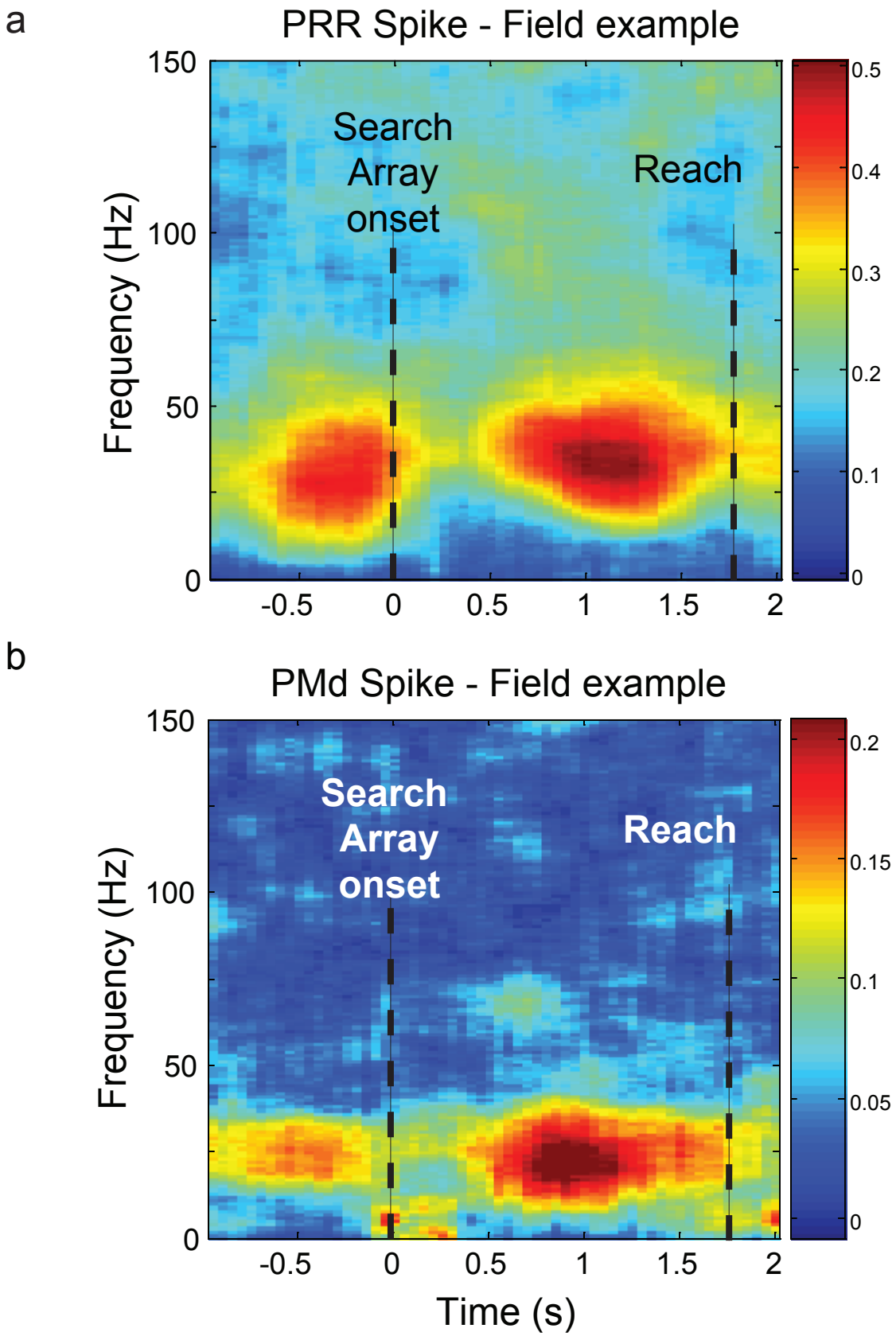

Supplementary Figure 7: Spike-field coherence within PRR and PMd during free search. **a**, Example spike-field coherence within PRR. **b**, Example spike-field coherence within PMd.

Supplementary Figure 8

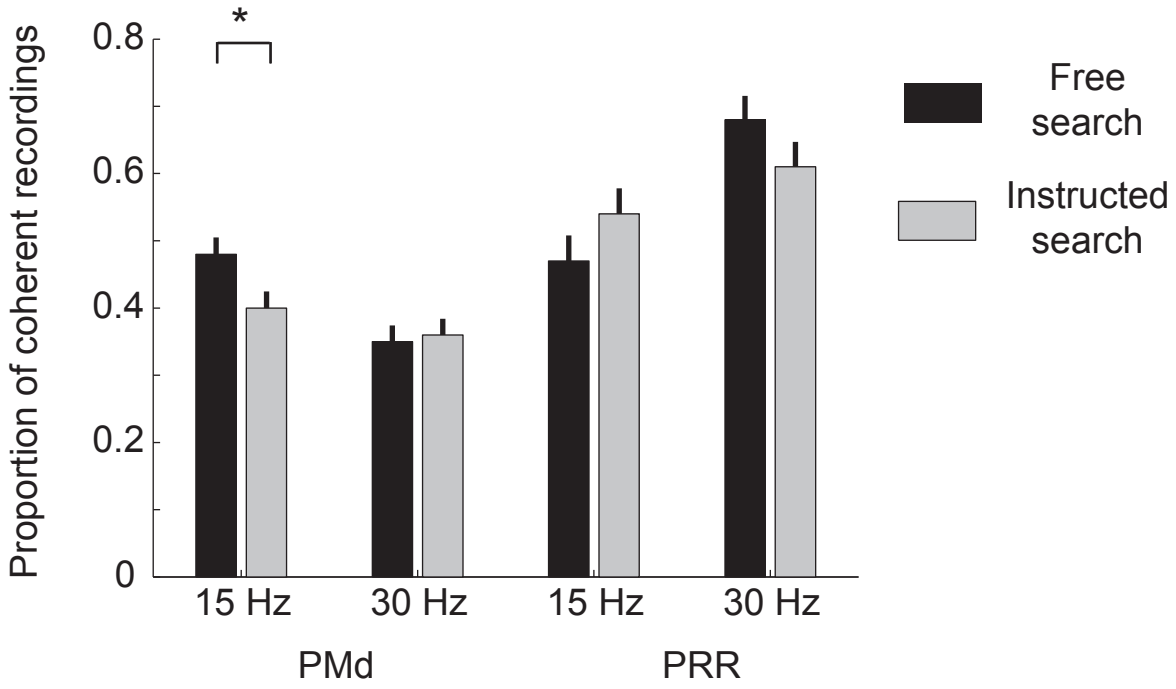

Supplementary Figure 8: Population analysis of spike-field coherence within PRR and PMd during free and instructed search. The proportion of recordings with significant 15 Hz coherence immediately following search array onset and significant 30 Hz coherence during the delay period are shown. Lines denote standard error of the mean for each proportion. * denotes statistically significant difference between free and instructed search, determined according to a chi-squared test, $p<0.05$. Analysis is based on 397 PMd spike-field recordings and 173 PRR spike-field recordings.

Supplementary Figure 9

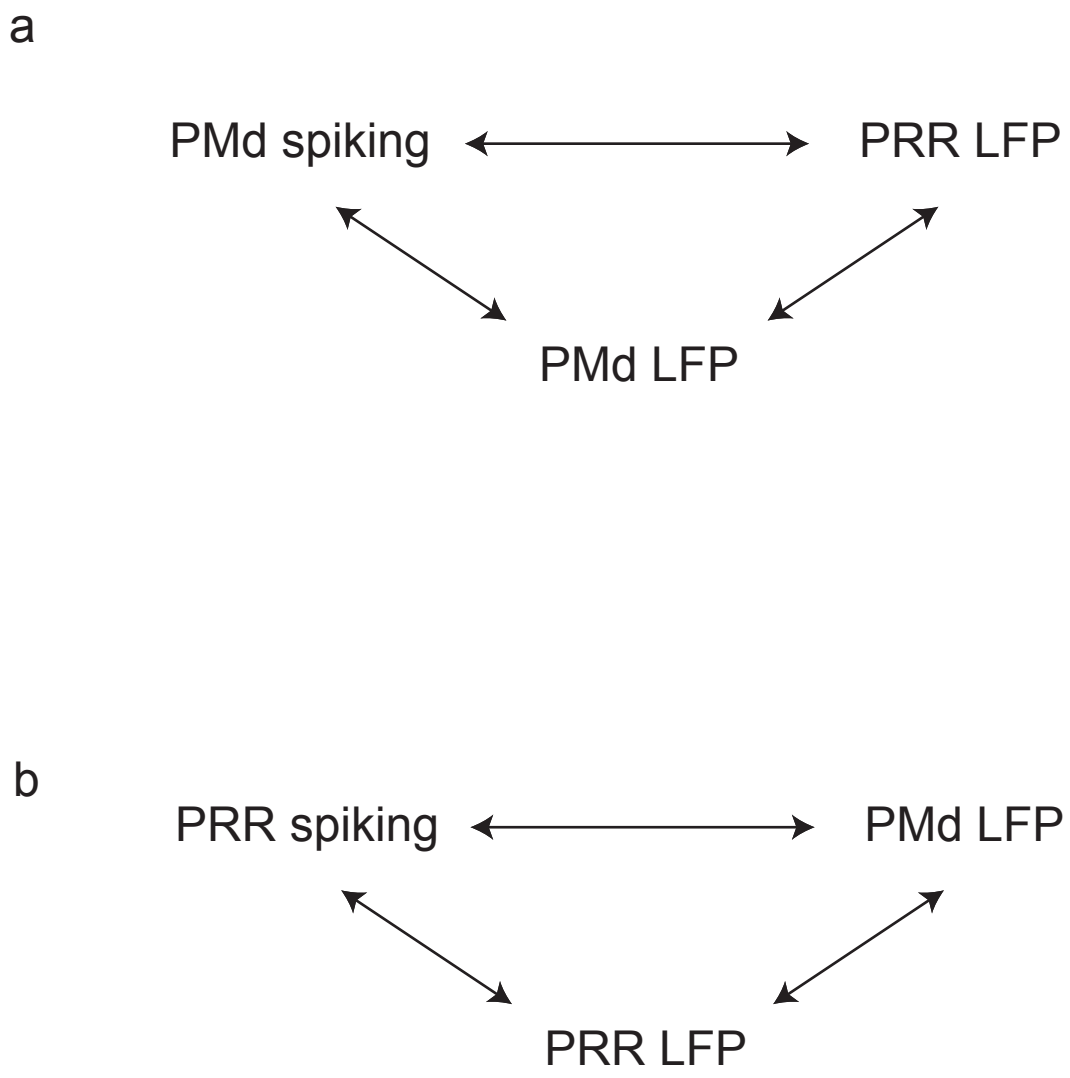

Supplementary Figure 9: Schematic for partial spike-field coherence analysis showing how spike-field coherence between PMd and PRR can be due to LFP activity in each area. Arrows denote coherence between any pair of measurements. **a)** PMd spiking is coherent with PRR LFP activity, as shown by the arrows along the top. However, PMd LFP activity is also coherent with PMd spiking as well as with PRR LFP activity, shown by arrows in the lower triangle. This means that we might expect some PMd spiking is coherent with PRR LFP activity as a result of the arrows in the lower triangle. Partial PMd spike – PRR field coherence is given by calculating PMd spike – PRR field coherence (upper arrows in triangle) and subtracting the PMd spike – PRR field coherence expected from PMd LFP activity (lower arrows in triangle. **b)** Analogous relationships for partial PRR spike – PMd field coherence.

Supplementary Figure 10

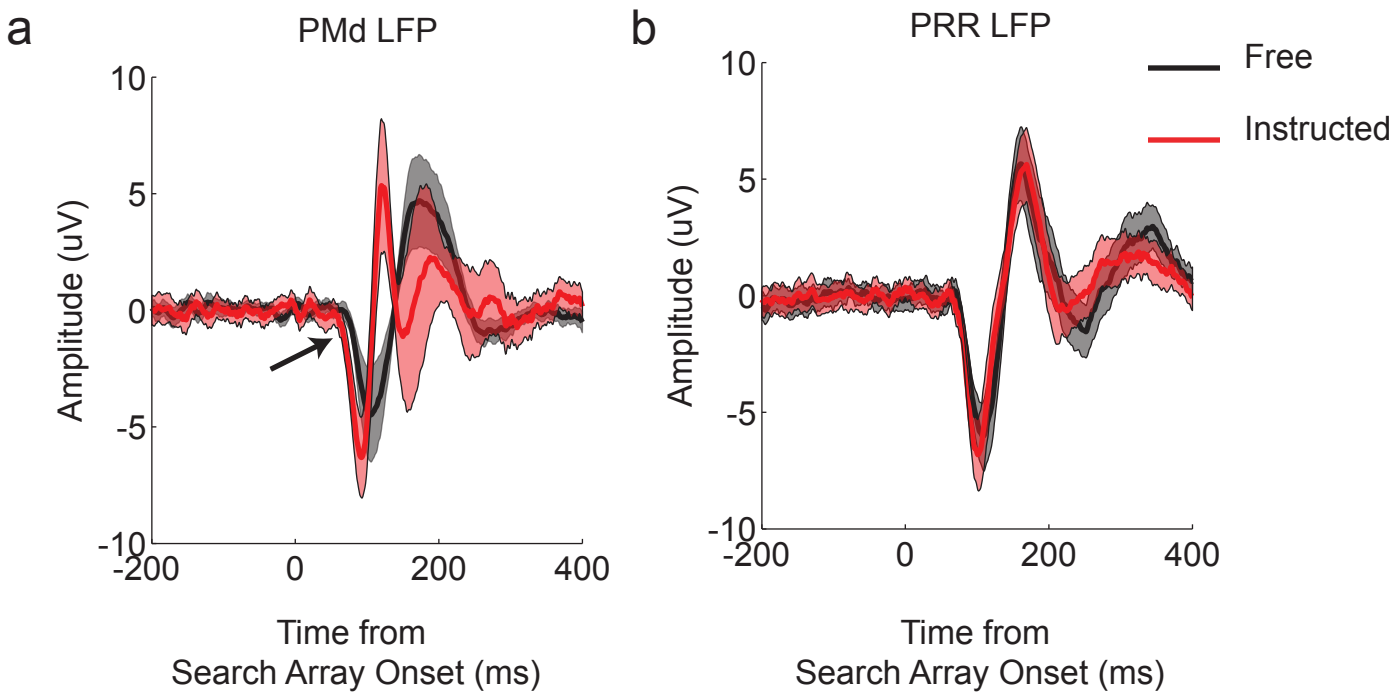

Supplementary Figure 10:LFP response latencies. **a**, Evoked PMd LFP response to search array onset during free search (black) and instructed search (red). Shaded regions give 95% confidence intervals. Arrow marks onset of significant difference between each response ($p<0.05$). **b**, Evoked PRR LFP response to search array onset, as above. There is no significant difference between each response.

Table 1: Population PMd spike – PRR field coherence during search tasks with enforced fixation

PMd Spike – PRR Field Coherence		
Free or Instructed		
30/111 (27%)		
Free only	Instructed only	Free and instructed
21/30 (70%)	4/30 (13%)	5/30 (17%)

Table 2: Population PRR spike – PMd field coherence during search tasks with enforced fixation

PRR Spike – PMd Field Coherence		
Free or Instructed		
17/58 (29%)		
Free only	Instructed only	Free and instructed
9/17 (53%)	1/17 (6%)	7/17 (41%)